U.PORTO

MESTRADO INTEGRADO EM MEDICINA

The fundamental principles of cell cycle control: what goes wrong with aging?

Ana Rita Carvalho Araújo

M

2023

Dissertação de conclusão do Mestrado Integrado em Medicina, submetida ao Instituto de Ciências Biomédicas Abel Salazar, Universidade do Porto.

Original article in preparation for publication

Title: The fundamental principles of cell cycle control: what goes wrong with aging?

Author: Ana Rita Araújo [1,2]
Estudante do 6º ano profissionalizante do Mestrado Integrado em Medicina, Instituto de Ciências Biomédicas Abel Salazar, Universidade do Porto; número de estudante: 200706563
Endereço eletrónico: up200706563@edu.icbas.up.pt

Orientadora: Doutora Elsa Logarinho [2]
Investigadora Principal no Instituto de Investigação e Inovação em Saúde (i3S) da Universidade do Porto

[1] Instituto de Ciências Biomédicas Abel Salazar, Universidade do Porto, Portugal

[2] i3S- Instituto de Investigação e Inovação em Saúde, Porto, Portugal.

Assinado por: **Ana Rita Carvalho Araújo**
Num. de Identificação: 13543574
Data: 2023.05.31 22:58:28 +0100

Ana Rita Carvalho Araújo

Elsa Clara Carvalho Logarinho Santos

Porto, Junho de 2023

“Scientific thought is fed by the capacity to 'see' things differently than they have previously been seen.”

– Ursula K. Le Guin, The Ones Who Walk Away from Omelas –

ACKNOWLEDGEMENTS

The work here presented was possible due to the support of my supervisor, Dr Elsa Logarinho. I am grateful for your teachings, undeniable support, trust and believing in these hypotheses.

To all past and current members of 208.S1 lab at i3S, as well as ALM and TraCy facilities, thank you for your help and encouragement. Being surrounded by great minds and great people really makes everything simpler and more joyful.

Lastly, I would like to thank the financial agencies that supported this work: Fundação para a Ciência e a Tecnologia I.P., in the framework of the projects EXPL/BIA-CEL/0446/2021, PTDC/MED-OUT/2747/2020 and by POCI-01-0145-FEDER-007274 framework project co-funded by COMPETE 2020 PORTUGAL 2020 through FEDER.

RESUMO

Tendo em conta a elevada incidência de doenças associadas ao envelhecimento prevista para as próximas décadas, é prioritário compreender o processo de envelhecimento a nível molecular, celular e fisiológico. O envelhecimento é caracterizado pela perda da capacidade regenerativa, embora se desconheça o modo como as células envelhecidas abrandam o seu ciclo celular, perdem a capacidade proliferativa e acabam por se tornar senescentes. Recentemente, foi descoberto que a repressão do fator de transcrição FoxM1, que possui papéis pleiotrópicos em proliferação, diferenciação e senescência celular, é responsável pelo declínio mitótico durante o envelhecimento devido a uma diminuição global da transcrição de genes mitóticos em células proliferativas. Num estudo independente, verificou-se que a mitose está temporalmente isolada da variabilidade das fases do ciclo celular em diferentes tipos celulares, sendo invariavelmente rápida devido à robustez do mecanismo de regulação feedback da atividade Cdk1-CyclinB1. Curiosamente, verificou-se um aumento de 1,5 vezes na duração do ciclo celular e da mitose nas células idosas, o que sugere que os limiares moleculares que controlam as transições de fase do ciclo celular se tornam desregulados e ineficientes com o envelhecimento. Numa abordagem multidisciplinar usando culturas celulares de fibroblastos derivados de dadores saudáveis com idades entre 0 e 87 anos como modelo celular *in vitro* de envelhecimento natural, foi possível perceber os perfis de expressão e a atividade de alguns dos principais intervenientes no ciclo celular - Cdk1, FoxM1 e o seu regulador APC/C-Cdh1. Estas moléculas estão interligadas através de mecanismos de feedback, demonstrando um importante impacto na perda de capacidade proliferativa e no aumento da senescência durante o envelhecimento. A modulação deste mecanismo de feedback mostrou que a repressão de Cdh1 em células idosas consegue restaurar a competência do ciclo celular e reduzir os níveis de senescência. Assim, o mecanismo de feedback Cdk1:APC/C-Cdh1:FoxM1 surge como um biomarcador e/ou alvo útil para futuras intervenções anti-envelhecimento.

Palavras-chave: Envelhecimento, Senescência, Ciclo Celular, Fibroblastos

ABSTRACT

Considering the high incidence of age-associated diseases expected in the next decades, it is a priority to understand the process of aging at molecular, cellular, and physiological levels. Aging is characterised by loss of regenerative capacity, though it remains elusive how aged cells slowdown cycling, lose proliferative capacity and ultimately become senescent. It was previously found that repression of the FoxM1 transcription factor, with pleiotropic roles in cell proliferation, differentiation and senescence, accounts for mitotic decline during aging due to a global transcriptional shutdown of mitotic genes in proliferating cells. In an independent study, mitosis was found to be temporally insulated from variability in earlier cell-cycle phases in distinct cell types due to the robustness of the positive feedback loop controlling Cdk1-Cyclin B1 activity. Intriguingly, there is a 1.5-fold increase in both cell cycle and mitosis durations in elderly cells, suggesting that molecular thresholds controlling cell cycle phase transitions become unfitted and sluggish with aging. A multidisciplinary approach combining live single-cell imaging of primary human dermal fibroblasts of advancing age donors with high-throughput image analysis showed that the expression profiles and activity of key cell-cycle players – Cdk1, FoxM1 and their regulator APC/C-Cdh1 – are entangled in a feedback loop that impacts into the loss of proliferative capacity and senescence accrual during aging. Modulation of this feedback loop showed that Cdh1 repression in elderly cells restored cell cycle fitness and reduced senescence levels. Thus, the Cdk1:APC/C-Cdh1:FoxM1feedback arises as a useful biomarker and/or target for future anti-aging interventions.

Keywords: Aging, Cellular Senescence, Cell Cycle, Fibroblasts

ABBREVIATIONS

APC/C	Anaphase promoting complex/Cyclosome
bs	Beam splitter
Cdh1/Fzr1	Cdc20 related 1/Fizzy-related protein
Cdk	Cyclin-dependent kinase
DAPI	4',6-diamidino-2-phenylindole
DMEM	Dulbecco's modified Eagle's medium
DMSO	Dimethyl sulfoxide
DNA	Deoxyribonucleic Acid
Dox	Doxycycline
em	Emission wavelength
ex	Excitation wavelength
FACS	Fluorescence-Activated Cell Sorting
FBS	Fetal Bovine Serum
FCS-H	Forward scatter area vs. Side scatter area
FoxM1	Forkhead Box M1
FSC-A	Forward scatter area
FUCCI	Fluorescent Ubiquitination-based Cell Cycle Indicator
HDFs	Human Dermal Fibroblasts
m	Slope of the trend line
mCherry	Monomeric red fluorescent protein
MEM	Minimal Essential Medium
mL	milliLitre
mM	milliMolar
MMB	MYB-MuvB complex
ms	miliseconds
NEB	Nuclear envelop breakdown
NER	Nuclear envelop reformation
nm	nanoMeter
nM	nanoMolar
OECdh1	Cdh1 overexpression
OEFoxM1	FoxM1 overexpression
PBS	Phosphate buffered saline

PBS-T	PBS + 0.05% Tween-20
pH3	Phospho-histone 3
PIP	PCNA-interacting protein
Plk-1	Polo-like kinase 1
r	Person correlation coefficient
R^2	Coefficient of determination
RNA	Ribonucleic Acid
rpm	Revolutions per minute
rTTA	Reverse tetracycline-controlled transactivator
s	second
SA-β-gal	Senescence-Associated β-galactosidase
SASP	Senescence-Associated Secretory Phenotype
SD	Standard Deviation
siRNA	small-interfering RNA
SAC	Spindle assembly checkpoint
SSA-A	Side scatter area
Wee1 inh	Wee1 inhibitor - PD0166285
YFP	Yellow fluorescent protein
µL	microLitre
µm	microMeter
µM	micromolar

CONTENTS

LIST OF FIGURES

1. INTRODUCTION

Today, 8.5% of people worldwide are aged over 65 and 1 in 5 people will be old-age in 2050 [1]. The unprecedented rate at which the world's elderly population is growing, is leading to significant burden on the healthcare systems of every country due to higher incidence of old-age co-morbidities such as cardiovascular, neurodegenerative and cancer diseases [2–4]. Therefore, it is a priority to understand the process of aging at molecular, cellular, and physiological levels to come out with comprehensive strategies for healthspan extension.

The hallmarks of aging have been proposed and among them, cellular senescence, a state of permanent cell-cycle arrest with several stereotypical features including the secretion of pro-inflammatory molecules (or SASP), has gained solid evidence for its contribution to aging and age-related diseases [5,6]. However, the mechanisms behind cell cycle slowdown in aged cells, the deregulation and/or changes in cell cycle core machinery network, error propensity, and ultimately senescence onset, remain poorly understood.

The decision to divide is one of the most fundamental cellular responses and the networks that control cell division can adapt and remodel in different biological contexts. The cell cycle is characterized by a sequence of events – G1-, S-, G2-phases and Mitosis – by which a cell gives rise to two daughter cells [7,8]. The fidelity of cell division depends on a complex regulatory network, which controls the timing and order of all cell cycle events [8]. Even though the molecular machinery that drives cell division cycles is common and evolutionary conserved in all tissues, it is known that distinct cell types exhibit very different cycles. In essence, progression through cell cycle is dependent on the activation and deactivation of cyclin-dependent kinases (Cdks) complexes and the switching between DNA duplication and DNA segregation in all cells [7,8]. Moreover, biochemical feedback loops keep transitions through cell cycle ordered and unidirectional, adding an extra layer of control to the cell cycle network [9,10].

All events in mitosis are driven by the activation of Cdk1-Cyclin B1 complex that is heavily regulated by positive feedback control [11–13]. It activates its own activator – Cdc25 [14,15]– and inhibits its own inhibitor – Wee1 [16–18]–, which creates a switch-like activation of Cdk1-Cyclin B1 and turns mitotic entry an explosive and irreversible decision (Figure 1A). It was previously demonstrated that mitotic duration is short, constant, and independent of variability of upstream cell cycle events in different cell types, from embryonic stem cells to differentiated and cancer cells. The mechanism underlying temporal insulation of mitosis is the positive

feedback loop at mitotic entry – Wee1:Cdk1-Cyclin B1:Cdc25 –, that when impaired, mitosis takes longer, becomes variable and coupled with previous cell cycle events [19]. Also, perturbing positive feedback not only compromises mitosis in mother cells but also affects successive daughter cell cycles. This demonstrates that a short and constant mitosis uncoupled from variability in upstream events is crucial for fidelity of cell division and fitness of subsequent cell cycles.

Interestingly, it was also recently shown that human dermal fibroblasts (HDFs) retrieved from skin biopsies of elderly donors, exhibit cell cycle slowdown, increased mitotic duration and a higher rate of mitotic defects [20]. It was disclosed that repression of Forkhead Box M1 (FoxM1) transcriptional activity is the determinant mechanism behind mitotic decline during aging leading to a global shutdown of mitotic genes in older cells [20]. First Cdk1-Cyclin A and later Cdk1-Cyclin B1 complexes phosphorylate FoxM1 that is subsequently recruited by the MYB-MuvB (MMB) complex to trigger the expression of late cell cycle genes that will drive G2-phase and Mitosis [21] (Figure 1B). In elderly mitotic cells there is a more than 2-fold reduction in the transcript and protein levels of major players of the positive feedback controlling mitotic entry, namely Cyclin B1, Plk1 and Cdc25C, which expression is modulated by FoxM1 transcriptional activity levels (Figure 1C). Moreover, FoxM1 activity is also under positive feedback regulation at G2/M transition, as FoxM1 is activated by Cdk1-Cyclin B1 and at the same it induces Cyclin B1 transcription to activate more Cdk1-CyclinB1 complexes [22,23]. By the end of mitosis, degradation of Cyclin B1 turns off Cdk1-Cyclin B1 activity, allowing for accumulation of the E3 ubiquitin ligase, APC/C-Cdh1, which drives FoxM1 degradation [24,25] (Figure 1D).

Lower FoxM1 levels have been related with cellular senescence and aging. FoxM1 expression is decreased in fibroblasts from middle-aged and elderly healthy donors, as well as in individuals with Hutchinson-Gilford progeria, a rare genetic disorder characterized by premature aging symptoms that occur at a young age [20]. However, its overexpression was able to rescue the expression of a comprehensive gene network comprising several senescence core signature genes and SASP genes [20,26,27]. APC/C-Cdh1 activity levels are kept low in undifferentiated human embryonic stem cells, driving short division cycles and, in contrast, post-mitotic neurons have high levels of Cdh1 and stay all their lives in a post-mitotic state, never re-entering the cell cycle [28,29]. Likewise, complete depletion of Cdh1 in cultured post-mitotic neurons led to a re-entry into S-phase and increased levels of Cyclin B1, followed by apoptotic cell death [30,31].

Together, these observations raise the hypothesis that the temporal insulation of mitosis might be lost in an aged cell cycle, meaning that mitosis becomes coupled with increased cell cycle

length, having an impact in the proliferative fitness of old cells. However, evidence for the causality that drives the cell cycle arrest with aging is limited. To tackle this hypothesis, human dermal fibroblasts (HDFs) collected from healthy Caucasian males with ages ranging from neonatal to octogenarian were used as an *in vitro* model to study cellular aging [20,32]. Using live-cell imaging, it was possible to dissect at single-cell level, how the cell cycle dynamics changes along advancing age. The cell cycle length increases steadily along aging, due to an increased duration of all cell cycle phases. The temporal insulation of mitosis is indeed lost with aging as a result of defective activation of Cdk1-Cyclin B1 complex at mitotic entry. Moreover, depletion of FoxM1 in young cells also leads to the loss of mitotic insularity, whereas mitotic insularity is rescued in old cells either by overexpressing FoxM1 or by depleting Cdh1. A longer cell division cycle is also observed in young cells upon Cdh1 overexpression, as well as the accumulation of senescence markers. In contrast, the Cdh1 depletion in aged cells results in a shorter cell cycle and a decrease of senescence markers, suggesting that the interlinked relationship between Cdk1, APC/C:Cdh1 and FoxM1 might play a causal role in age-related cell cycle frailty and senescence accrual.

2. MATERIALS AND METHODS

2.1. Cell Culture

All cell stocks were routinely tested for mycoplasma and were cultured at 37ºC and humidified atmosphere with 5% CO_2. Human fibroblasts established from skin samples of reported "healthy" Caucasian males with ages ranging from neonatal to octogenarian (neonatal, DFM021711A, ZenBio Biobank; 10-year-old, GM03348, Coriell Cell Repository; 21-year-old, GM23964, Coriell Cell Repository; 42-year-old, AG06235, Coriell Cell Repository and 87-year-old, AG10884, Coriell Cell Repository) were cultured in Minimal Essential Medium (MEM) with Earle's salts and L-glutamine (10-010-CV, Corning), supplemented with 15% Fetal Bovine Serum (FBS) (Gibco) and 1x Antibiotic-Antimycotic (Gibco). Only early passage dividing fibroblasts (up to passage 3–5) were used. To produce lentiviruses, HEK293T cells were used and were cultured in Dulbecco's modified Eagle's medium (DMEM) (Gibco) supplemented with 10% FBS (Gibco) and 1x Antibiotic-Antimycotic (Gibco).

2.2. Lentiviral Generation and Biosensors

To generate pLVX–Tight-Puro–Cdh1, a *Not*I–Cdh1–*EcoR*I fragment was amplified from HA-cdh1 Addgene plasmid (Catalog no. #11596) with primers Fw:5'ATATAGCGGCCGCATGGACCAGGACTATGAGC3' and Rv:5'ATATAGAATTCTTACCGGATCCTG GTGAAG3'. The fragment was then inserted into pLVX–Tight-Puro (Clontech) digested with *Not*I + *EcoR*I.

HEK293T helper cells were transfected with packaging plasmids pMd2.G and psPAX2 using Lipofectamine 2000 (Life Technologies) to generate lentiviruses carrying pLVX–Tight-Puro–Cdh1, pCSII-EF1a-CyclinB1-YFP (kindly provided by Dr. Silvia Santos [11]), pLenti-PGK-Neo-PIP-FUCCI [33] (Addgene #118616, kindly provided by Dr. Jorge Ferreira) or pLVX–Tight-Puro–FOXM1-dNdK [20]. Virus-containing media was collected 48 hours after transfection. Media was removed from HEK293T cells and spun down at 2400 rpm for 5 minutes. The virus-containing supernatant was aliquoted and snap-frozen using liquid nitrogen before storage at -80ºC. HDFs were infected for 6 hours in the presence of 8 μg/mL polybrene (AL-118, Sigma-Aldrich, MO, USA). In the case of pLVX–Tight-Puro–Cdh1 and pLVX–Tight-Puro–FOXM1-dNdK, cells were co-infected with the

responsive and the reverse tetracycline-controlled transactivator (rTTA) lentiviruses at a ratio 2:1. In the following day, 500ng/mL of doxycycline (D9891, Sigma-Aldrich, MO, USA) was added to the medium to induce co-transduction. Phenotypes were analysed and quantified 72 hours after induction. Regarding pCSII-EF1a-CyclinB1-YFP and pLenti-PGK-Neo-PIP-FUCCI cells were sorted one week after infection in a FACS Aria II cell sorter (BD Biosciences) using an 85µm nozzle and the blue (488nm) and yellow/green (561nm) lasers. Cells were gated by forward scatter area (FSC-A) vs. side scatter area (SSA-A) and FSC-A vs. FSC-height (FCS-H) plots to exclude dead cells and doublets/clumps, respectively. The sorting gates were designed accordingly to the respective auto-fluorescent control.

2.3. siRNA knockdown

Cells were plated in serum-depleted culture medium and, after 1 hour, transfected either with 50 nM FoxM1 small interfering RNA (siRNA) (SASI_Hs01_00243977 from Sigma-Aldrich, MO, USA), or with 25nM fzr1/Cdh1 small interfering RNA (siRNA) (M-015377-01 from Dharmacon). Transfections were performed using Lipofectamine RNAiMAX in Opti-MEM medium (both from Gibco) according to the manufacturer's instructions. Transfection medium was replaced by complete medium after 6 hours. Phenotypes were analysed and quantified 72 hours after transfection for siFoxM1 and 48 hours for sifzr1/Cdh1.

2.4. Immunofluorescence

Cells were seeded 2-3 days before fixation in 96-well ibidi plates (Catalog no. #89626). Cells were rinsed twice in Phosphate buffered saline (PBS) before fixation with 4% paraformaldehyde in PBS for 10 minutes at room temperature. Cells were washed 3 times for 5 minutes with PBS before permeabilization in PBS with 0.3% Triton X-100 at room temperature for 7 minutes. Cells were then washed 3 times with PBS-T (PBS + 0.05% Tween-20) and incubated with blocking buffer containing 10% FBS in PBS-T for 1 hour at room temperature. Cells were incubated overnight at 4ºC with primary antibodies diluted in PBS-T + 5% FBS as follows: mouse anti-fzr1 (#SC-56312, Santa Cruz Biotechnology, CA, USA) 1:75, rabbit anti-53BP1 (#4937, Cell Signalling Technology, MA, USA), 1:500; mouse anti-p21 (#SC-6246, Santa Cruz Biotechnology, CA, USA), 1:800; rabbit anti-FoxM1 (#13147, ProteinTech Group, Inc., IL, USA), 1:500; anti-Ki67 (8D5,

#9449, Cell Signalling), 1:500; anti-p16INK4a (#ab7962, Abcam), 1:200; rabbit anti-pH3 (#06-570, Millipore). After being washed 3 times with PBS-T, cells were incubated with secondary antibodies Alexa Fluor-488 and/or Alexa Fluor-568 (Life Technologies) diluted 1:1000 in PBS-T + 5% FBS for 1 hour at room temperature. Nuclei were stained using DAPI (Sigma-Aldrich, MO, USA) 1µg/mL.

2.5. SA-β-gal activity assay

Live cells were incubated for 90 minutes in medium with 100 nM Bafilomycin A1 (B1793, Sigma-Aldrich, MO, USA) to induce lysosomal alkalinization. Fluorogenic substrate (33 µM) for β-galactosidase, fluorescein di-β-D-galactopyranoside (F2756, Sigma-Aldrich, MO, USA) was then added to the medium, and incubation carried out for 90 minutes. Cells were then fixed in 4% paraformaldehyde for 15 minutes, rinsed with PBS once and permeabilized with 0.1% Triton-X100 in PBS for 15 minutes. Nuclei were stained using DAPI (Sigma-Aldrich, MO, USA) 1µg/mL.

2.6. Live-cell and Fixed-cell Microscopy

Live cell imaging was performed on either an inverted motorized Leica Timelapse DMI6000B (Leica Microsystems) or in an inverted motorized Nikon ECLIPSE TI widefield microscope (Nikon) equipped with the Hamamatsu Orca-FLASH4.0 sCMOS (C11440, Hamamatsu) or Andor iXon Ultra 888 EMCCD (Andor) camera, respectively, both with temperature, humidity, and CO_2 controls to maintain the sample integrity. Leica Timelapse DMI6000B (Leica Microsystems) images were acquired with an HCX PL FLUOTAR L 20x/0.40 Corr Ph1, using a binning 2x2 and a 16-bit depth, exposure time of 20ms with a lamp intensity of 20. Images were acquired every 10 minutes for 72 hours. The microscope was controlled through the LAS X software (version 3.8.1.26810) using the navigation tool “LAS X Navigator”.

When using the Nikon ECLIPSE TI, fluorescence images were acquired with a Plan Apo λ 20x/0.75 DIC N2 objective. To excite the YFP the Lumencor Spectra X Teal – 510/25 nm was used in combination with the following filter set cube: CFP/YFP - ex 416/501 - bs 440/520 - em 464/547, using a LED % of 10 and an exposure time of 150ms. For mCherry, the Lumencor Spectra X Green – 550/15 was used with LED % of 15, an exposure time of 200ms, in combination with the following filter set cube:DAPI/FITC/TRITC/Cy5 – Pinkel Quad (FF410/504/582/669/Di01).

Brightfield images were acquired with exposure time of 10ms with a lamp intensity of 5V. Images were acquired using binning 2x2 and a 16-bit depth.

For live-cell imaging experiments, cells were seeded in 96-well or 24-well ibidi plates (Catalog no. #89626 and #82426, respectively), on the day before the experiment, to avoid induced synchronicity of the cell cycle after splitting. In a typical experiment to follow cell cycle dynamics, cells were monitored from 48 to 120 hours, with images taken every 10 minutes. In experiments where positive feedback at mitotic entry was perturbed using the Wee1 inhibitor PD166285 (Sigma) at 3µM/mL, and DMSO as control, cells were imaged for 5 hours after adding the inhibitor (or DMSO), with images taken every 4 minutes with the same acquisition conditions.

For fixed-cell immunostaining analyses, cells were imaged in the inverted motorized Leica DMI6000B widefield microscope (Leica Microsystems) equipped with Hamamatsu Orca-FLASH4.0 sCMOS (C11440, Hamamatsu), and 40x objective, a Leica EL6000 light source (metal-halide lamp) and controlled through the LAS X software (version 3.8.1.26810). Samples were imaged using a binning 2x2. DAPI acquisition was done using the following filter cube set: AT – ex: 340-380; bs: 400; em: LP 425, with FIM at 100%, and an exposure time of 20ms. For Alexa-488 l the filter cube set L5 – ex: 460/40; bs: 505; em: 527/30 was used, with FIM at 100% and an exposure time of 1s, and for Alexa-568 the TX2 filter cube set was used: ex: 560/40; bs: 660; em: 700/75, using FIM at 100% and an exposure time of 1s.

2.7. Image analysis

Live-cell movies and fixed-cell experiments were blindly quantified using ImageJ/Fiji software.

2.8. Statistical analysis

All experiments were repeated at least two times. Sample sizes and statistical tests used for each experiment are indicated in the respective figure captions. Data are shown as mean ± SD. GraphPad Prism version 8 was used to analyse all the data. Data were tested for parametric versus non-parametric distribution using D'Agostino–Pearson omnibus normality test. Mann-Whitney U test, two-tailed Fisher's exact test and two-sided Kruskal-Wallis with Dunn's multiple comparison correction tests were then applied accordingly to determine the statistical

differences between different groups (*$p < 0.05$, **$p < 0.01$, ***$p < 0.001$, ****$p < 0.0001$, and *ns* not significant $p > 0.05$).

3. RESULTS

3.1. The cell cycle length increases with aging

To measure cell cycle dynamics along aging, HDFs retrieved from different donors with age ranging from neonatal to octogenarian, and expressing the PIP-FUCCI sensor, were imaged for two consecutive divisions (Figure 2A,B) [33–36]. The duration of different cell cycle phases was measured as follow: G1-phase length was monitored by the appearance and disappearance of Cdt1-PIP-venus; S-phase length was defined as the time between appearance of Geminin-mCherry and re-appearance of Cdt1-PIP-venus at beginning of G2-phase; G2-phase was measured by monitoring the time between the re-appearance of Cdt1-PIP-venus and nuclear envelope breakdown (NEB), which was characterised by observing the localisation of both biosensors; and finally mitosis was defined by the time between NEB and nuclear envelope reformation (NER). Total cell cycle length was measured as the time between two consecutive NER events.

The cell cycle length was determined for HDFs derived from individuals with different ages, increasing gradually with aging. The cell cycle of age-range HDFs is 13.3±2.2 hours for neonatal cells, 16.5±5.0 hours for 10-year-old cells, 19.2±7.5 hours for 21-year-old cells, 22.3±9.5 hours for 42-year-old cells and 24.1±10.0 hours for 87-year-old cells (Figure 2C). In terms of temporal cell cycle dynamics, neonatal cells spent 4.2±1.9 hours in G1-phase, 6.5±0.9 hours in S-phase, 1.9±0.6 hours in G2-phase and 35.4±7.2 minutes in mitosis; 10-year-old cells spent 6.7±4.4 hours in G1-phase, 6.5±1.1 hours in S-phase, 2.4±0.9 hours in G2-phase and 40.2±5.6 minutes in mitosis; 21-year-old cells spent 8.6±7.3 hours in G1-phase, 7.5±2.5 hours in S-phase, 2.4±0.5 hours in G2-phase and 42.6±5.4 minutes in mitosis; 42-year-old cells spent 10.9±9.0 hours in G1-phase, 7.3±1.2 hours in S-phase, 3.2±1.4 hours in G2-phase and 49.2±8.4 minutes in mitosis; and 87-year-old cells spent 11.9±9.4 hours in G1-phase, 8.1±2.8 hours in S-phase, 3.3±1.2 hours in G2-phase and 55.2±9.6 minutes in mitosis (Figure 2D). These results showed that increased duration of all cell cycle phases accounts for the overall cell cycle slowdown along aging.

3.2. Duration of mitosis becomes steadily correlated with cell cycle length along aging

In a previous study, the positive feedback at mitotic entry was shown to keep duration of mitosis short, constant, and insulated from variability in earlier cell-cycle events, and that if disrupted, mitosis becomes considerably longer and variable in individual cells [19]. Since mitotic duration was found to increase with aging (Figure 2D), this raised the question if temporal insulation of mitosis is lost in older cells. To test this hypothesis the time between two consecutive NER events was measured as cell cycle length, and the time between NEB and NER was defined as the duration of mitosis, again in a range of HDFs derived from different donors.

In the case of HDFs derived from young donors – neonatal and 10-year-old cells – mitosis was uncoupled from previous cell cycle events (Pearson correlation coefficient, *r* – neonatal=0.001, 10-year-old=0.07) (Figure 2E). 21-year-old cells showed a mild correlation between cell cycle length and mitosis (*r*=0.30) and cells derived from older donors, 42-year-old and 87-year-old, showed a striking correlation between mitotic duration and cell cycle length (*r*=0.38 and *r*=0.47, respectively). This experiment strongly indicates that positive feedback at mitotic entry is compromised along aging and that mitosis is not temporally insulated from variability in upstream cell cycle events in older cells. Mitotic duration becomes steadily dependent of, and coupled with, cell cycle duration in older cells.

3.3. The switch-like activation of Cdk1 is compromised in older cells

Mitotic entry is initiated by a bistable trigger that activates Cdk1, which is thought to be the basis for a unidirectional and irreversible entry and progression through mitosis [11–13,37]. In addition, the presence of positive feedback regulation in the activation of Cdk1 gives rise to an explosive and sharp activation of Cdk1, as well as a short and constant mitotic duration. Contrary to what was previously described [19], elder cells exhibit longer and more variable mitosis, that is coupled with cell cycle length, suggesting that the positive feedback at mitotic entry is not working properly, compromising the switch-like activation of Cdk1. Taken these observations altogether, it was asked if the switch-like activation of Cdk1 is different in young vs. old cells, being more graded in the latter (Figure 3A).

neonatal and 87-year-old cells stably expressing Cyclin B1-YFP biosensor were used to test this hypothesis (Figure 3B). Cyclin B1 nuclear translocation was used as a proxy of Cdk1 activation, since its nuclear translocation depends on direct phosphorylation by Cdk1 that is crucial for Cyclin B1 redistribution at onset of mitosis [11,19,38,39]. To quantitatively measure Cdk1 activation, time courses of Cyclin B1 redistribution in individual cells were fitted to the logistic equation and rise times were calculated from the curve fits for all cells. As expected, Cdk1 activation in neonatal cells was illustrated by a sharp sigmoidal curve, typical of an explosive activation (left panel of Figure 3D), with a fitted rise time of 2.5±1.1 minutes. However, in 87-year-old cells, the sharpness of the curve was lost (right panel of Figure 3D). In elder cells, Cdk1 activation showed an increased rise time of 6.0±5.1 minutes, supporting the idea that Cdk1 is activated in a more sluggish way.

3.4. Older cells are less prone to enter a new round of mitosis than younger cells

Since older cells take more time to reach mitosis and spend longer periods in interphase, next it was investigated how prone are older cells to undergo mitosis. To this end, live-cell imaging of freely cycling HDFs was performed in the presence or absence of a mitotic trigger. Wee1 inhibitor (PD166285) was used as a "mitotic trigger", releasing Cdk1 from Wee1 inhibition and facilitating entry into mitosis (Figure 1A). After stimulation with the mitotic trigger, cells were imaged for five more hours to observe what happens to the cells when they receive a signal to enter mitosis.

Within 5 hours, 22% of control neonatal cells entered mitosis and this percentage decreases along aging with only 4.5% of 87-year-old cells dividing within the same time (Figure 3E). Upon stimulation with Wee1 inhibitor, 64.8% of neonatal cells were able to respond to the mitotic trigger. In contrast, only 16.7% of 87-year-old cells were able to go into mitosis. Moreover, this non responsiveness to the mitotic trigger increases progressively with aging with 55.5% of 10-year-old cells, 21.2% of 21-year-old cells and 16.8% of 42-year-old cells responding to the Wee1 inhibitor and entering mitosis. These results showed that cells can in fact be pushed into mitosis when stimulated with a mitotic trigger, but this competence decreases with aging.

3.5. FoxM1 repression disrupts the temporal insulation of mitosis from upstream cell cycle events

Repression of FoxM1 was established as the molecular mechanism behind mitotic decline during aging [20], leading to transcriptional shutdown of major players of the positive feedback controlling Cdk1 activation, cell cycle length and mitosis duration. All together, these findings suggest that the expression levels of major cell cycle feedback regulators show a different profile in elderly vs. young cells, with FoxM1 repression during aging accounting for the loss of mitotic insularity. Thus, FoxM1 was siRNA-depleted in young cells to determine if it was possible to replicate the aged phenotype in young cells, turning mitosis dependent on cell cycle length. Conversely, overexpression of FoxM1 through lentiviral infection in old cells was used to determine if this could rescue mitotic insularity (Figure 4A). When compared with control, neonatal siFoxM1-depleted cells exhibited a mitotic delay (57.0±10.8 minutes in siFoxM1 cells vs. 43.2±6.6 minutes in control cells) and spent more time in the cell cycle (25.1±8.2 hours in siFoxM1 cells vs. 18.4±3.5 hours control cells). The opposite was observed when FoxM1 was overexpressed (OEFoxM1) in 87-year-old cells. Both mitotic duration (42.6±5.9 minutes in OEFoxM1 cells vs. 55.8±17.4 minutes control cells) and cell cycle length (20.7±3.2 hours in OEFoxM1 cells vs 24.2±10.2 hours in control cells) decreased when a constitutively active truncated form of FoxM1 was expressed in 87-year-old cells. As shown before, mitosis was insulated in neonatal controls and coupled with cell cycle length in 87-year-old cells (Pearson correlation coefficient, r – neonatal=0.04 and 87-year-old=0.57). However, siRNA-mediated depletion of FoxM1 in neonatal cells recapitulated the coupling between cell cycle length and mitotic duration observed in old cells (r=0.54). At the same time, 87-year-old OEFoxM1 cells were able to rescue mitosis uncoupling from cell cycle length (r=0.03). This experiment demonstrated that FoxM1 repression is responsible for the loss of the temporal insulation of mitosis with aging.

3.6. Cdh1 levels increase with FoxM1 depletion in young cells and increase with aging

It was shown above that the duration of both mitosis and cell cycle increase with aging, and the same phenotype is also present when FoxM1 levels are suppressed in young cells. Moreover, FoxM1 activity is regulated by the activity of APC/C-Cdh1 and since when APC/C-Cdh1 is on,

FoxM1 activity is off, and vice-versa, this suggests that an increase of Cdh1 levels along aging could account for FoxM1 repression during aging. Previous RNA-seq data showed that elderly mitotic cells have 2-fold higher transcript levels of Cdh1/fzr1 [20] and indeed, when FoxM1 is depleted in neonatal cells, there is an increase in Cdh1/fzr1 levels compared with control (Figure 4B). In agreement, a gradual increase in Cdh1 levels was observed with advancing age, concomitantly to the gradual decrease in FoxM1 levels [20] (Figure 4C).

These results, together with the fact that FoxM1 is activated by Cdk1-Cyclin B1 and APC/C-Cdh1 is the proteolytic regulator of FoxM1, bring to question if a feedback regulation between Cdk1:APC/C-Cdh1:FoxM1 provides the link to explain FoxM1 repression during aging. To tackle this, modulations of Cdh1 expression were performed, both by overexpressing Cdh1 in neonatal cells and depleting Cdh1 in elderly cells, to understand the impact in FoxM1 levels, cell cycle length, proliferative capacity, and senescence accrual (Figure 5).

3.7. Overexpression of Cdh1 in young cells leads to loss of proliferative capacity and senescence accrual

Next, neonatal cells were lentiviral-transduced with a doxycycline-inducible Cdh1 construct and treated with 500ng/mL of doxycycline for 3 days, after which the levels of Cdh1 were measured by immunofluorescence. The levels of Cdh1 were 5-fold higher in transduced neonatal cells (OECdh1) vs. control (Figure 6A,B), whereas the levels of FoxM1 decreased in OECdh1 cells to levels equivalent to those previously reported for 87-year-old cells [20] (Figure 6A,C). As expected for FoxM1 repression, both mitotic and proliferative indexes were decreased in OECdh1 cell cultures, whereas the levels of senescence markers were increased (Figure 6D-H). Together these results suggest that higher levels of Cdh1 can account for a loss of proliferative capacity and senescence onset.

Then it was questioned what would be the effect of overexpressing Cdh1 on the cell cycle dynamics. For that, neonatal cells were treated with doxycycline for (to induce Cdh1 overexpression) and subsequently imaged for 72 hours to follow two consecutive division cycles. Whereas neonatal control cells (without doxycycline) spent 43.8±6.6 minutes in mitosis and took 12.8±1.4 hours to complete a whole cell division cycle (Figure 6I,J), neonatal cells overexpressing Cdh1 spent 50.4±7.2 minutes in mitosis and took 23.7±6.9 hours to complete the cell cycle.

Interestingly, overexpression of Cdh1 in neonatal cells, was able to disrupt the temporal insulation of mitosis, since the mitotic duration became correlated with total cell cycle length (Pearson correlation coefficient, r=0.30), which was not observed in neonatal control cells (Pearson correlation coefficient, r=0.04) (Figure 6K). In sum, overexpression of Cdh1 in neonatal cells is sufficient to remodel their cell cycle dynamics so that it resembles the dynamics of an aged cell cycle.

3.8. Cdh1 repression in elderly cells rescues senescence and restores cell cycle dynamics

Next, it was tested whether younger phenotypes could be also rescued in 87-year-old cells by conversely downregulating Cdh1 expression with small interference RNA (siRNA). A 25% depletion of Cdh1 levels was enough to perform the following experiments without compromising the fidelity of the cell cycle (Figure 7A). Regarding FoxM1 expression levels, they duplicated in Cdh1-depleted 87-year-old cells when compared with Mock control cells (Figure 7B). Moreover, depletion of Cdh1 was able to increase the mitotic index and the proliferative capacity of 87-year-old cells, and to decrease the levels of senescence markers (Figure 7C-G).

When compared with 87-year-old Mock cells, mitotic duration decreased in Cdh1-depleted 87-year-old cells from 45.6±9.6minutes to 41.4±7.2minutes (Figure 7H). The same was also observed in cell cycle length, with a decrease from 22.2±6.9 hours in 87-year-old Mock cells to 16.18±4.4 hours in Cdh1-depleted 87-year-old cells (Figure 7I). Finally, it was tested whether depletion of Cdh1 in old cells could restore mitosis insularity from the cell cycle. Indeed, 87-year-old Cdh1-depleted cells exhibited a Pearson correlation coefficient of r=0.007 vs. r=0.65 observed in Mock controls (Figure 7J). Altogether, the results revealed that Cdh1 levels have an impact on cell proliferation and fitness.

4. DISCUSSION

Most chronic diseases have aging has the major risk factor, due to the accumulation of senescent cells [40]. Fibroblasts are considered key players in senescence accrual as they represent a proliferative non-parenchymal subpopulation within tissues that is, therefore, likely to stop cycling in response to stressful conditions. Fibroblasts are part of the stroma, a supporting or connective tissue that provides support for the architecture and function of the parenchyma. The loss of functional and proliferative capacity of fibroblasts, impairs tissue remodelling and replacement of non-functional parenchymal cells, propagating the decrease of tissue function and ultimately organ failure [2–4,41–44].

Owing to the resolution of PIP-FUCCI sensor microscopy, this study shows that fibroblasts' cell cycle length gets longer with aging due to the slowdown of the overall cell cycle dynamics. It was found at single-cell level, that not only mitotic duration increases with aging, but also all the other cell cycle phases. Within all cell cycle phases, G1-phase duration is the one that increases the most and its lengthening correlates with advancing age. In fact, during development, the lengthening in G1-phase that happens upon differentiation marks the time where cells lose their high proliferative capacity, where cell cycle remodels, gets longer and gap phases are defined [45–47]. One of the characteristics of embryonic cells is self-renewal, so cells are programmed to divide repeatedly. In contrast, an important goal of cells in a somatic tissue is to keep division very controlled by ensuring correct replication and repair of DNA before segregation of the sister chromatids to maintain tissue integrity and stability. In line with this, it is possible that as the cells age, they enlarge their cell cycle to keep genome fidelity and avoid replication errors that can give rise to aberrant and dysfunctional cells, ultimately leading to organ failure.

Over the years, different models that are not mutually exclusive have been proposed to explain how cell cycle events are timely controlled and ordered [48–60]. And among them, the quantitative model for cell cycle progression claims that oscillations in Cdk-Cyclin complexes activity are sufficient to drive the cell cycle in an orderly and unidirectional manner [54,55,61], with Cdk2 activation initially driving S-phase and Cdk1 activation driving mitosis later on. Cell cycle length increases gradually with advancing age which might indicate that elder cells need more time to reach Cdk2 and Cdk1 activation thresholds to enter S-phase and mitosis [62–65], respectively, possibly due to slower activation of these major cell cycle drivers. Based on this hypothesis and in the observation that mitotic duration increases with aging [20], Cdk1 activation profile was

measured in both young and old cells. And indeed, the typical abrupt activation profile of Cdk1 at mitotic entry is not present in elderly cells, which suggests that the positive feedback loop at mitotic entry is compromised in old cells [11–13]. Instead, Cdk1 becomes activated in a more graded way, which supports the hypothesis that old cells need more time to reach key cell cycle thresholds, in this case, the threshold to enter mitosis. Compromising the rapid activation and nuclear import of Cdk1-Cyclin B1 has been previously shown to affect progression through mitosis [39,66,67], which also supports an increased mitotic duration along aging. Moreover, it was also possible to tackle the relationship between mitosis and cell cycle length that is known to have impact in the proliferative performance of daughter cells [19]. The insulation of mitotic duration is present in young cells and is steadily lost with aging. Additionally, it was also shown that the ability to respond to a strong mitotic trigger is steadily lost with increasing aging, with old cells having difficulties to commit to a new round of mitosis. This further supports the hypothesis that the quantitative model of cell cycle regulation applies along aging, with older cells taking more time to reach the adequate levels of molecular players to progress through the different cell cycle phases (Figure 8).

This study also aimed to understand which molecular players are determinant on cell cycle remodelling with aging. Since FoxM1 repression was found as the major driver of mitotic decline and loss of fidelity with aging, it was explored if its overexpression in old cells and its shutdown in young cells would rescue or disrupt, respectively, the temporal insulation of mitosis. And indeed, it was found that FoxM1 expression is required to keep mitosis temporally insulated from upstream cell cycle events, reinforcing the importance of FoxM1 expression and function to drive accurate and proper mitosis which impacts in the proliferative capacity of daughter cells [19]. Since FoxM1 is activated by Cdk1-Cyclin B1 and APC/C-Cdh1 is the proteolytic regulator of FoxM1 [24,25], it was then asked if a feedback regulation between these players provides the link to explain FoxM1 repression during aging. High Cdh1 levels were reported in FoxM1-depleted young cells, and advancing age correlated with increased Cdh1 levels. Modulation of Cdh1 levels led to the disclosure that overexpression of Cdh1 in young cells recapitulates phenotypes observed for elder cells, such as decreased FoxM1 levels and loss of proliferative capacity. These results were further corroborated by accelerated accumulation of senescence markers in young cells overexpressing Cdh1, including increase in p21/53BP1 levels, p16 levels and lysosomal mass [68–71]. The exact opposite was observed, when Cdh1 was depleted in older cells, where there was a rescue in FoxM1 levels, proliferative capacity, and delayed senescence. Before, it was shown that depletion of Cdh1 in cultured post-mitotic cells led to a re-entry into the cell cycle which further supports that high Cdh1 levels act as a cell cycle breaker sustaining a cell cycle arrest

state [30,31]. Finally, it was observed that high Cdh1 levels are enough to disrupt the mitotic insulation of mitosis in young cells, while its depletion in elderly cells rescues the mitotic insularity, causally linking Cdh1 depletion to FoxM1 expression, preventing senescence accrual and driving cell proliferation. APC/C-Cdh1 is also an important regulator of Cdk1-Cyclin B1 complex and is known that APC/C activity is reduced in embryonic stem cells allowing the fast Cdk1 activity oscillations [72]. Moreover, the activity of APC/C-Cdh1 increases during the differentiation of human embryonic stem cells [28]. This fosters the idea that the cell cycle might remodel twice during the life of an individual: when the cells transit from a pluripotent state to a differentiated state [73] and later in life to an aging state.

Overall, the results here presented showed that 1) Cdk1 activation, which alone can drive almost all cell cycle events is compromised with aging, 2) FoxM1 levels are important to keep mitotic duration insulated from earlier cell cycle phases, with FoxM1 repression accounting for the loss of mitotic insularity along aging and 3) Cdh1 levels rise with increasing age having an impact in cell cycle slowdown and appearance of senescence features. High Cdh1 levels result in longer cell division cycles, with FoxM1 levels being maintained lower during longer periods of time and being unable to induce the transcription of cell cycle drivers such as cyclin B1, that is important to activate Cdk1 and progress through the cell cycle. In contrast, low Cdh1 levels allow the faster accumulation of FoxM1, which will lead to the transcription and rapid increase in late cell cycle genes, activating Cdk1 in an all-or-none manner and driving a unidirectional cell cycle progression, without further delays. All these three players – Cdk1, FoxM1 and Cdh1 – regulate each other and these new findings disclosed a new feedback loop whose strength can determine the loss of proliferative capacity along aging. In young and elderly cells, the machinery that controls cell division is the same and only by changing the feedback strength between Cdk1, FoxM1 and Cdh1 it gives rise to fundamentally different cell division cycles. Modulating feedback strength may be a simple regulatory strategy that allows cells to fine-tune the period of division cycles and the feedback regulation of Cdk1 is here highlighted once more as playing a crucial role on it. Changing the strength of a feedback loop is a resource-inexpensive strategy to maintain cell integrity and function and could possibly explain the evolutionary conservation of the players of cell cycle control machinery across all cell types, independently of cellular context [74–76]. The increased strength of this feedback loop with aging, might be a way to prevent non fitted cells to progress through the cell cycle and propagate errors and anomalies, leading to tissue and organ dysfunction, more propensity to chronic diseases and ultimately organismal failure.

5. CONCLUSION

Overall, here it was unveiled which are the major changes in cell cycle dynamics that occur as cells age and important insight was provided into the thus far elusive deregulated cell cycle mechanisms accounting for loss of proliferative capacity and increased senescence features during aging. Moreover, it also highlights the importance of feedback loop regulation in the aged cell cycle. Feedback loops are simple and ubiquitous motifs that can define how genes and proteins regulate each other's and can bring about amplification, maintenance, and rapid switching of activities in time and space and be the basis for unidirectional, coherent, and all-or-none cellular events [10,66,77–81]. Here is presented evidence that modulating the strength of feedback regulation is enough to change the oscillatory frequency and velocity of cell division, adding an extra role that feedback loops play to regulate the cell cycle.

These results also expand our knowledge regarding how aging arises at molecular level, with loss of proliferation capacity and cellular fitness behaving like the kick-off pieces in a falling line of dominoes. Additionally, it enhances the importance of cell cycle fitness improvement as a senostatic strategy [20,27,32], as opposed to the mainstream senolytic therapies [82–85] that might disrupt beneficial functions of senescence such as tissue-repair [86–89]. This further supports the therapeutic potential for organismal healthspan extension which is crucial to cope with the socio-economic impact of the rapidly increasing aged population and associated chronic diseases, turning a priority to ensure healthy lives, and promoting the well-being at all ages.

6. APPENDIX 1 – Figures

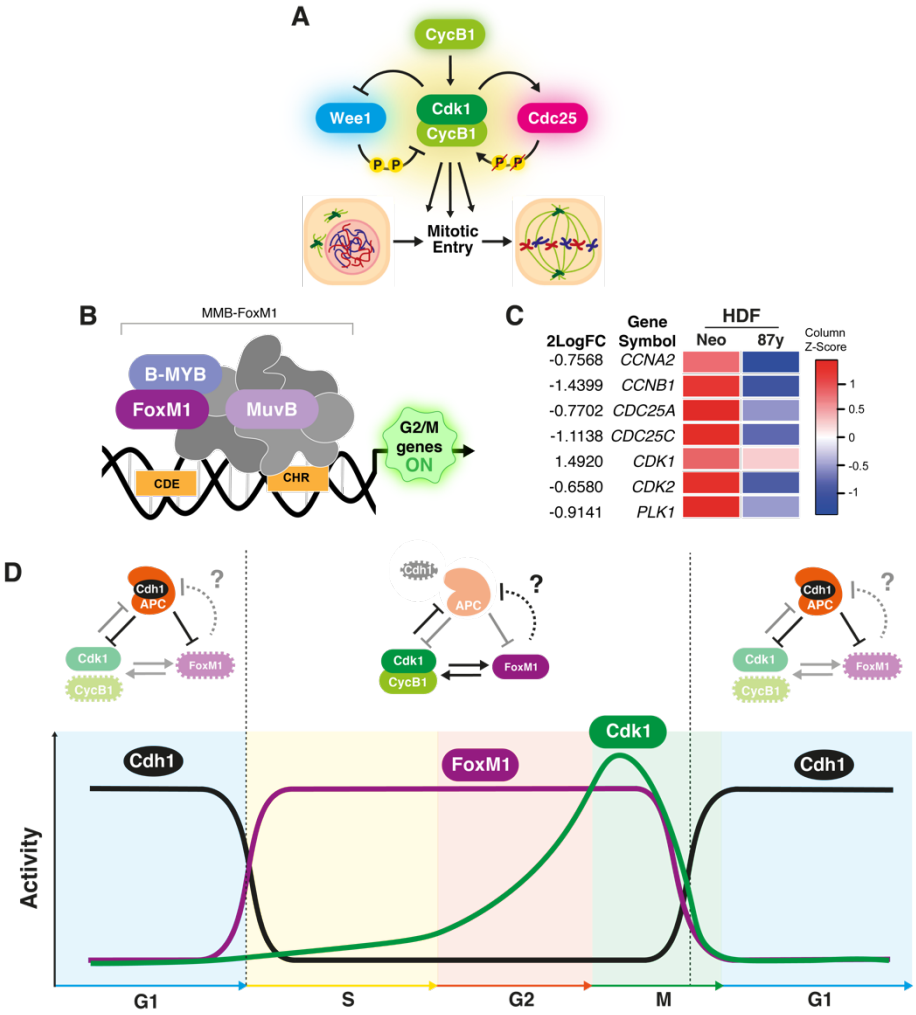

Figure 1. Positive feedback at mitotic entry and hypothesis that changes in feedback regulation between Cdk1:APC/C-Cdh1:FoxM1 account for decreasing proliferative rate along aging. ***A.*** Wiring diagram showing a simplified Cdk1-Cyclin B1 regulatory network at mitotic entry, including positive feedback loops with its main regulators Cdc25 and Wee1. ***B.*** Transcriptional regulation of G2/M genes by the FoxM1-MMB complex binding to CDE/CHR promoter elements. ***C.*** Heatmap of genes within the "mitosis" GO term differently expressed between neonatal and 87-year-old (87y) fibroblasts [20]. ***D.*** Interactions between Cdk1, APC/C-Cdh1 and FoxM1 and a possible new feedback loop that can regulate cell division time. At G1-phase, the major function of the E3 ubiquitin ligase APC/C and its co-activator Cdh1 is to keep low Cdks activity by degradation of S-phase and mitotic Cyclins until a cell commits to a new division cycle. Also, the transcriptional activity of FoxM1, that primarily drives the expression of cell division genes, is kept low by APC/C-Cdh1 proteolytic targeting of FoxM1. At G1/S-phase transition, Cdh1 is inactivated and degraded, concomitantly with the activation of Cdk-Cyclin complexes and FoxM1. In late S-phase and during G2-phase, FoxM1 is initially phosphorylated by Cdk1 and subsequently by Plk1, activating FoxM1 transcriptional activity that in turn leads to enhanced expression of key mitotic regulators that are crucial to drive a successful mitosis. Within these mitotic regulators is Cyclin B1 that will activate more Cdk1 to drive mitotic entry and progression through mitosis. Late stages of mitosis require Cdk1-Cyclin B1 inactivation by the APC/C complex that is kept inactive by the spindle assembly checkpoint (SAC) machinery until all the chromosomes are perfectly attached to the spindle microtubules and aligned along the metaphase plate. After satisfaction of SAC requirements, the Cdc20 co-activator of APC/C, which was sequestered by SAC players, is released to bind APC/C and initiate proteolytic activity required for mitotic exit. At this point in mitosis, high levels of Cdk1-Cyclin B1 will activate more APC/C-Cdc20 complexes, that in turn will target Cyclin B1 for degradation to turn off Cdk1 activity and exit mitosis. Low Cdk1 activity allows the replacement of Cdc20 by the Cdh1 co-activator, thereby providing substrate specificity required to maintain G1-phase.

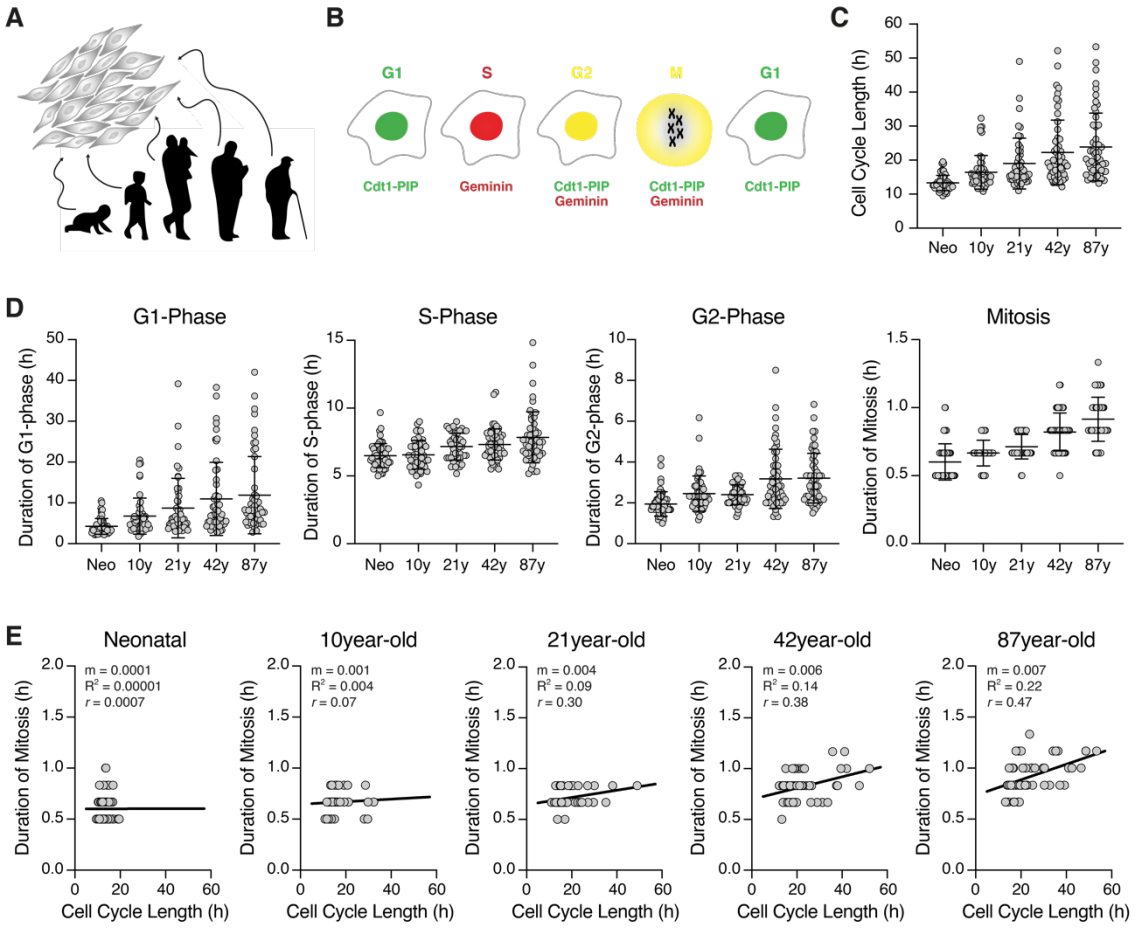

Figure 2. Mitotic duration becomes steadily correlated with cell cycle length along aging. ***A.*** *In vitro* model of cellular aging. Early passage human dermal fibroblast (HDF) cultures established from skin biopsies of different age donors. ***B.*** PIP-FUCCI genetically encoded fluorescence sensor that enables real-time monitoring of cell-cycle dynamics [33]. ***C.*** Cell cycle length measured by the time between two consecutive mitoses in neonatal, 10-, 21-, 42- and 87-year-old HDFs. Mean ± SD are shown as bars. ***D.*** Duration of G1-phase, S-phase, G2-phase, and mitosis measured by single live-cell imaging in neonatal, 10-, 21-, 42- and 87-year-old HDFs expressing the PIP-FUCCI biosensor. Mean ± SD are shown as bars. ***E.*** Duration of mitosis measured by the time between nuclear envelope breakdown (NEB) and nuclear envelope reformation (NER) as a function of cell cycle duration in neonatal, 10-, 21-, 42- and 87-year-old HDFs. The trend lines with respective slope (*m*), R-squared (R^2), and Pearson coefficient (*r*) are shown. n>50 cells, ≥2 independent experiments.

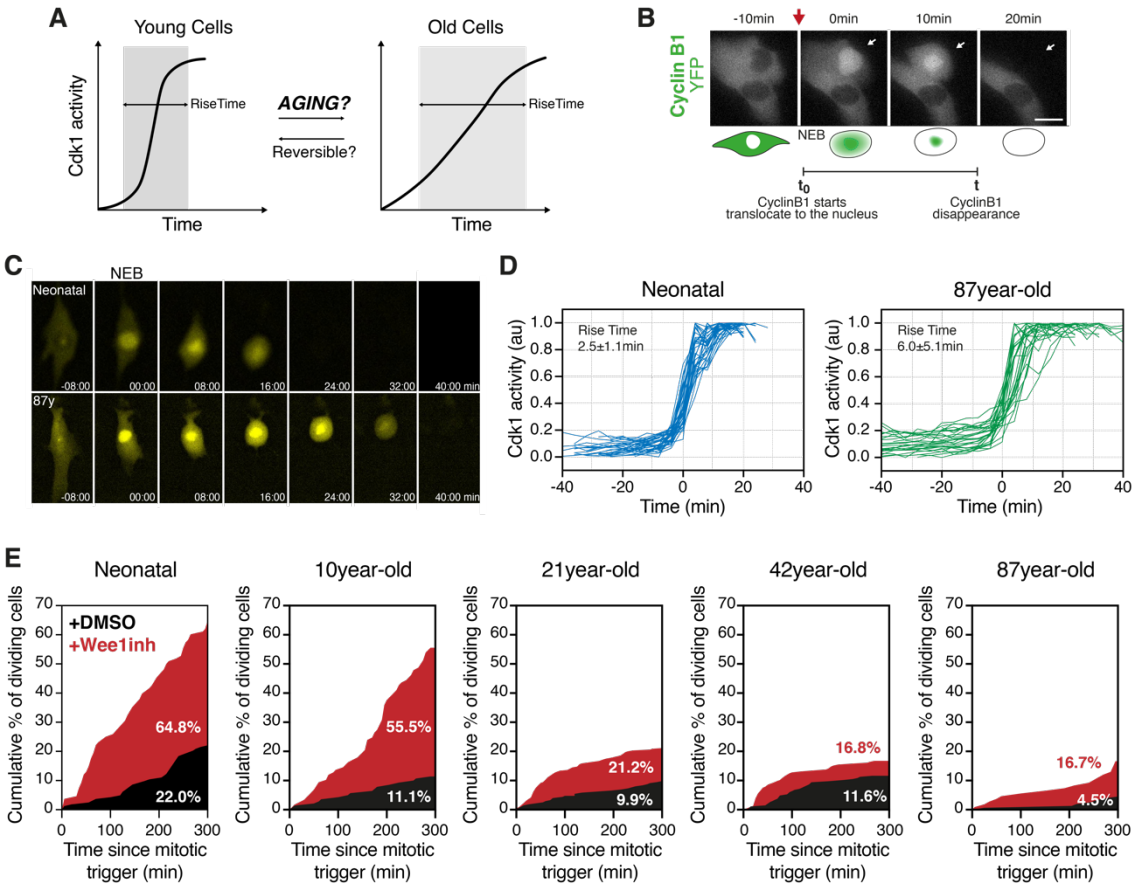

Figure 3. Switch-like activation of Cdk1 is compromised in older cells. ***A.*** Schematic of the experimental design to test whether positive feedback at mitotic entry is deregulated during aging. The hypothesis is that the sharp sigmoidal activation of Cdk1 at mitotic entry (left) is lost as the cell ages and mitotic entry becomes more sluggish (right). ***B.*** Representative images showing how Cdk1 activity was measured using Cyclin B1 biosensor. Red arrow marks the beginning of mitosis. White arrows mark the cell that was followed. Scale bar, 10 µm. Bottom: schematic of the appearance of the Cyclin B1 biosensor during mitosis. ***C.*** Representative images showing nuclear translocation of Cyclin B1 as a proxy for Cdk1 activity in neonatal (top panel) and 87-year-old (bottom panel) cells. ***D.*** Quantification of Cdk1 activity over time in neonatal (left panel) and 87-year-old (right panel) cells. Individual time courses were fitted to the logistic equation $y=a+b/1+e-(t-t_0/\tau)$ and were scaled to their fitted maximum and minimum values (b and a, respectively) and half-maximal times (t_0). Rise times (τ) were calculated from the curve fits for all cells and are expressed as Mean ± SD (n>40 cells). ***E.*** Cumulative percentage of dividing cells as a function of time following treatment with mitotic trigger in neonatal, 10-, 21-, 42- and 87-year-old HDFs. Cells were either treated with DMSO (black) or with Wee1 inhibitor (Wee1 inh) (red) (n>100 cells, 2 independent experiments).

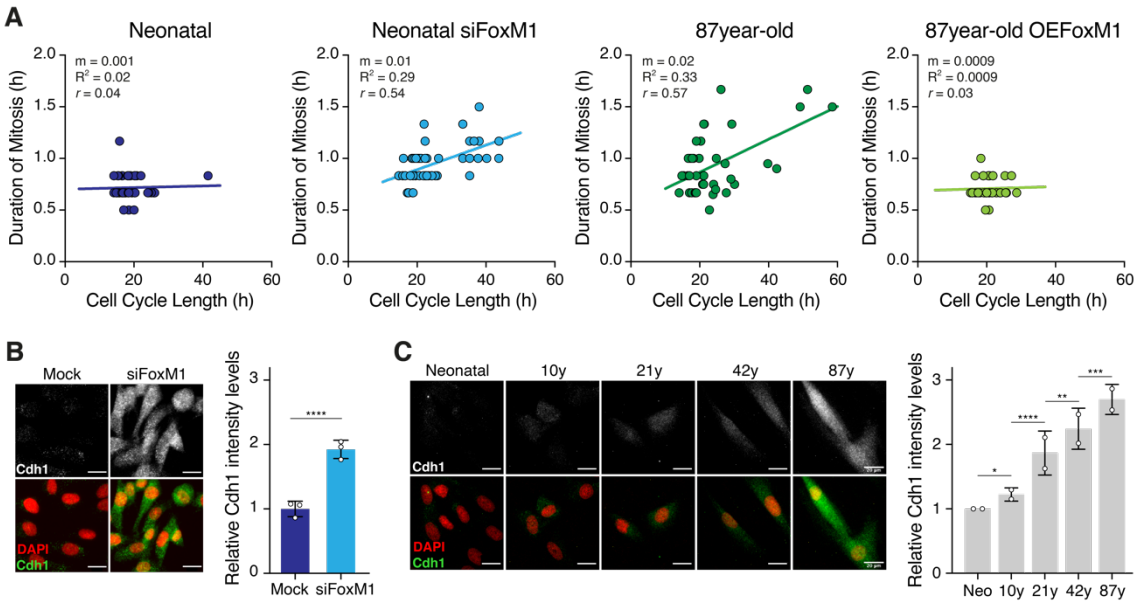

Figure 4. siRNA-mediated depletion of FoxM1 in neonatal cells recapitulates the coupling between cell cycle length and mitotic duration observed in 87-year-old HDFs. ***A.*** Duration of mitosis (measured by the time between NEB and NER) as a function of cell cycle length in neonatal cells, FoxM1-depleted neonatal cells (siFoxM1), 87-year-old cells and 87-year-old cells overexpressing FoxM1 (OEFoxM1). The trend lines with respective slope (*m*), R-squared (R^2), and Pearson coefficient (*r*) are shown. n>50 cells, ≥2 independent experiments. ***B.*** Representative images and quantification of Cdh1 intensity levels by immunofluorescence analysis of neonatal cells (Mock) and FoxM1-depleted neonatal cells (siFoxM1). Levels were normalized to Mock condition. n≥330 cells, 3 independent experiments. ***C.*** Representative images and quantification of Cdh1 intensity levels by immunofluorescence analysis of neonatal, 10-, 21-, 42- and 87-year-old HDFs. Levels were normalized to neonatal condition. n≥250 cells, 2 independent experiments. **p-value*≤0.05, ***p-value*≤0.01, ****p-value*≤0.001, *****p-value*≤0.0001 by Mann-Whitney U test (B) and two-sided Kruskal-Wallis with Dunn's multiple comparison correction (C). All values represent mean ± SD. Scale bar: 20 µm.

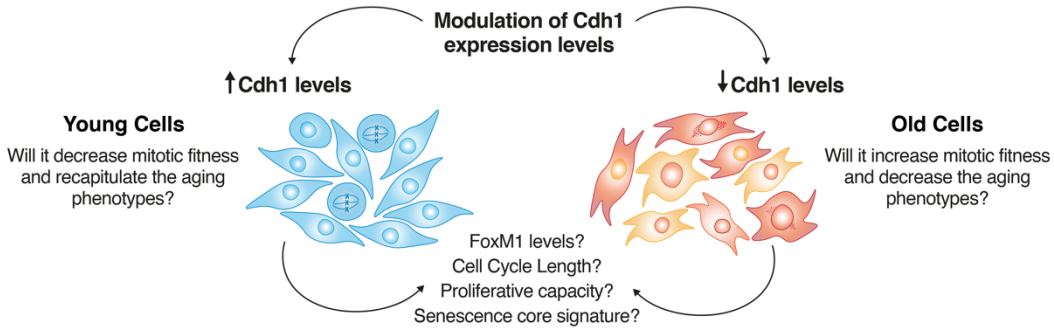

Figure 5. Rationale on how modulation of Cdh1 could lead to the disclosure of a new feedback loop controlling cell proliferation vs. cell senescence. High Cdh1 levels will be induced in young cells and at the same time Cdh1 levels will be repressed in old cells. The aim of these modulations is to access their impact in FoxM1 levels, cell cycle time, proliferation capacity and senescence markers.

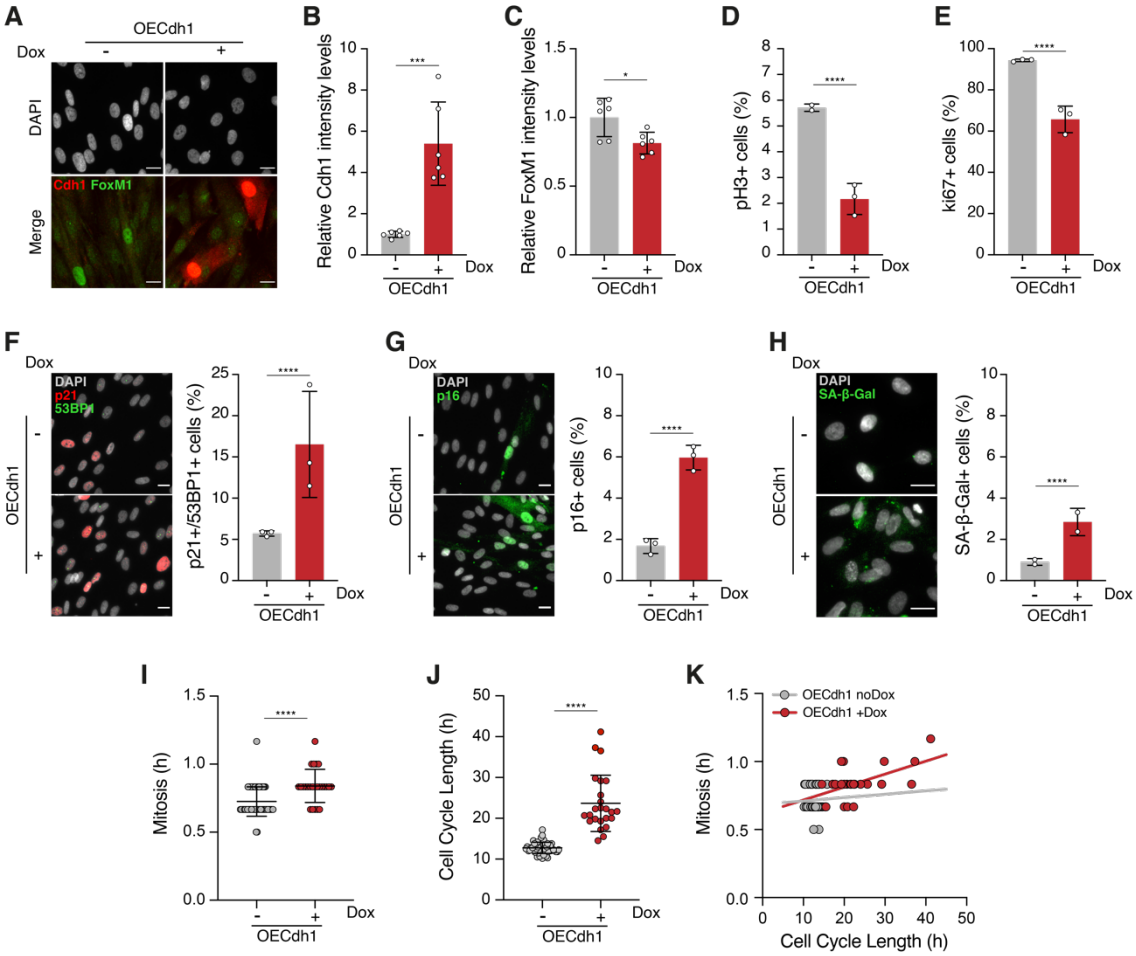

Figure 6. Overexpression of Cdh1 in young cells reproduces aged cells' phenotypes. ***A-C.*** Representative images *(A)* and quantification of Cdh1 (*B)* and FoxM1 (*C*) intensity levels by immunofluorescence analysis in neonatal control (-Dox) or overexpressing Cdh1 (+Dox) cells. Levels were normalized to neonatal control (-Dox) condition. n≥550 cells, 6 independent experiments. ***D*** Percentage of mitotic cells (positive for phospho-histone 3 immunostaining – pH3+) in neonatal control (-Dox) or overexpressing Cdh1 (+Dox) cells. n≥2000 cells, ≥2 independent experiments. ***E.*** Quantification of ki67+ proliferating cells. n≥3000 cells, 3 independent experiments. ***F.*** Representative images and quantification of cells staining positive for double immunostaining of p21 (cell cycle inhibitor) and 53BP1 (≥ 1 foci; DNA damage) senescence biomarkers in neonatal control (-Dox) or overexpressing Cdh1 (+Dox) cells. n≥3000 cells, 3 independent experiments. ***G.*** Representative images and quantification of cells staining positive for p16 senescence marker in neonatal control (-Dox) or overexpressing Cdh1 (+Dox) cells. n≥3000 cells, 3 independent experiments. ***H.*** Representative images and quantification of cells staining positive for SA-β-gal activity assay in neonatal control (-Dox) or overexpressing Cdh1 (+Dox). n≥3000 cells, 3 independent experiments. ***I.*** Mitotic duration and ***J.*** Cell cycle length measured in neonatal control (-Dox) or overexpressing Cdh1 (+Dox) cells. n>50 cells, 2 independent experiments. ***K.*** Duration of mitosis measured by the time between NEB and NER as a function of cell cycle length in neonatal cells, neonatal control (-Dox) or overexpressing Cdh1 (+Dox) cells. The trend lines with respective slope (*m*), R-squared (R^2), and Pearson coefficient (*r*) are shown. n>50 cells, 2 independent experiments. **p-value*≤0.05, ****p-value*≤0.001, *****p-value*≤0.0001 by Mann-Whitney U test (B and C) and two-tailed Fisher's exact test (D, E, F, G and H). All values represent Mean ± SD. Scale bar: 20 µm.

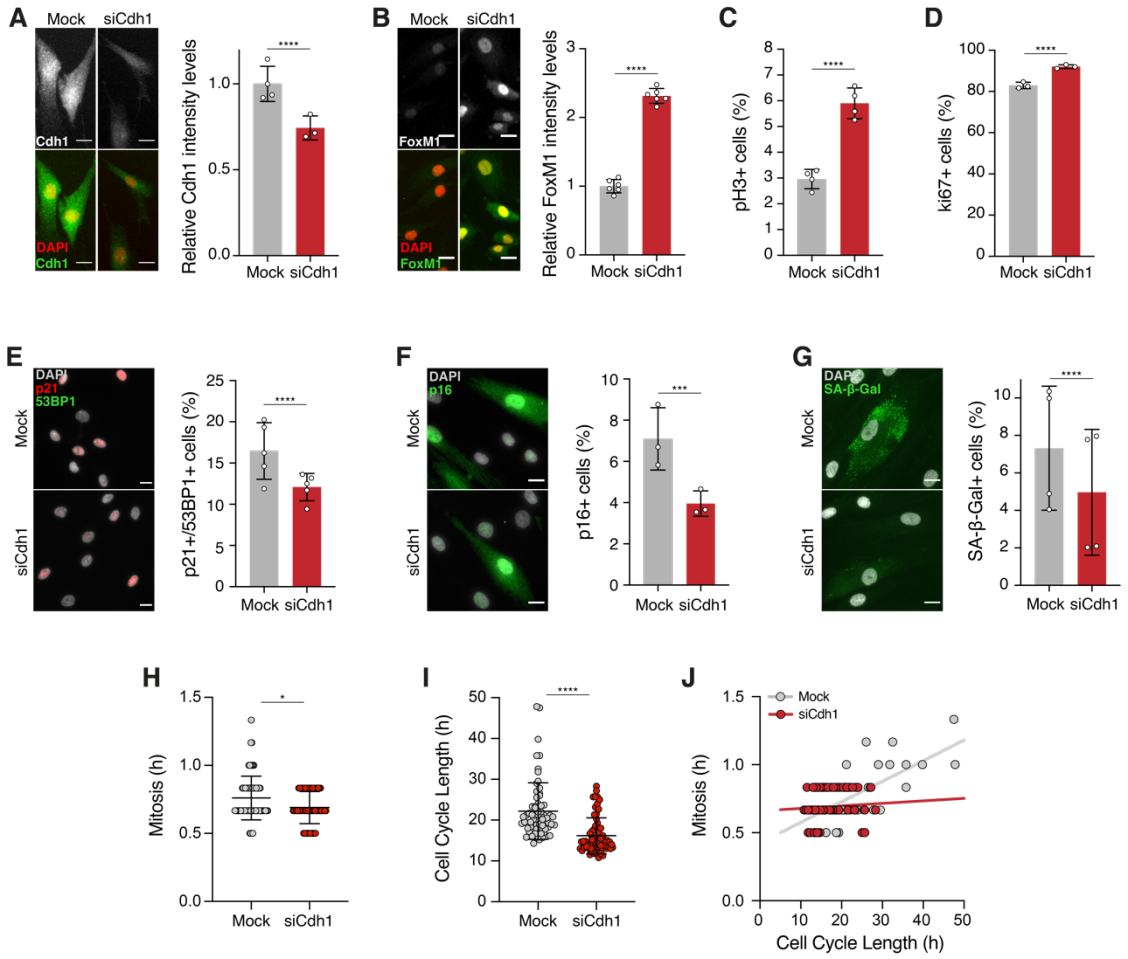

Figure 7. siRNA-mediated depletion of Cdh1 in elderly cells rescues senescence and restores cell cycle dynamics. ***A.*** Representative images and quantification of Cdh1 intensity levels by immunofluorescence analysis in 87-year-old control (Mock) and Cdh1-depleted (siCdh1) cells. Levels were normalized to Mock condition. n≥200 cells, ≥3 independent experiments. ***B.*** Representative images and quantification of FoxM1 intensity levels by immunofluorescence analysis in 87-year-old Mock and siCdh1 conditions. Levels were normalized to Mock condition. n≥800 cells, 6 independent experiments. ***C.*** Percentage of mitotic cells (positive for phospho-histone 3 immunostaining – pH3+) in 87-year-old Mock and siCdh1 conditions. n≥4000 cells, 4 independent experiments. ***D.*** Quantification of ki67+ proliferating cells in 87-year-old Mock and siCdh1 conditions. n≥3000 cells, 3 independent experiments. ***E.*** Representative images and quantification of cells staining positive for double immunostaining of p21 (cell cycle inhibitor) and 53BP1 (≥ 1 foci; DNA damage) senescence biomarkers in 87-year-old Mock and siCdh1 conditions. n≥2500 cells, 5 independent experiments. ***F.*** Representative images and quantification of cells staining positive for p16 senescence marker in 87-year-old Mock and siCdh1 conditions. n≥1500 cells, 3 independent experiments. ***G.*** Representative images and quantification of cells staining positive for SA-β-gal activity assay in 87-year-old Mock and siCdh1 conditions. n≥2000 cells, 4 independent experiments. ***H.*** Mitotic duration (time between NEB and NER) and ***I.*** cell cycle length measured in 87-year-old Mock and siCdh1-depleted cells. n>60 cells, 2 independent experiments. ***J.*** Duration of mitosis as a function of cell cycle length in 87-year-old Mock siCdh1-depleted cells. The trend lines with respective slope (*m*), R-squared (R^2), and Pearson coefficient (*r*) are shown. n>60 cells, 2 independent experiments. **p-value*≤0.05, ****p-value*≤0.001, *****p-value*≤0.0001 by Mann-Whitney U test (A and B) and two-tailed Fisher's exact test (C, D, E, F and G). All values represent Mean ± SD. Scale bar: 20 µm.

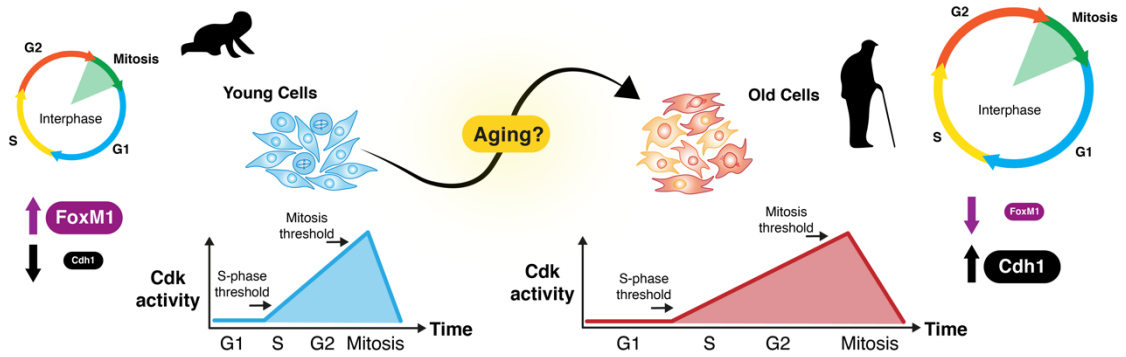

Figure 8. Changes in the Cdk1:APC-Cdh1:FoxM1 feedback regulation contribute to loss of proliferative capacity and FoxM1 repression during aging. Model summarizing the hypothesis that cell cycle slowdown with concomitant loss of proliferative capacity with aging is due slower attainment of Cdks thresholds.

7. REFERENCES

1. United Nations, Department of Economic and Social Affairs, Population Division. (2020) World Population Ageing 2019 - Highlights (ST/ESA/SER.A/444).
2. Pawelec G, Goldeck D, Derhovanessian E. Inflammation, ageing and chronic disease. *Curr Opin Immunol*. 2014;29(1):23-28.
3. Kennedy BK, Berger SL, Brunet A, et al. Geroscience: Linking aging to chronic disease. *Cell*. 2014;159(4):709-713.
4. Trumble BC, Schneider-Crease I. Chronic diseases of aging in an evolutionary context. *Evol Med Public Health*. 2020;2020(1):84-85.
5. López-Otín C, Blasco MA, Partridge L, Serrano M, Kroemer G. Hallmarks of aging: An expanding universe. *Cell*. 2023;186(2):243-278.
6. López-Otín C, Blasco MA, Partridge L, Serrano M, Kroemer G. The hallmarks of aging. *Cell*. 2013;153(6):1194-1217.
7. Maller JL, Gautier J, Langan TA, et al. Maturation-promoting factor and the regulation of the cell cycle. *J Cell Sci*. 1989;12:53-63.
8. Morgan DO. *Cell Cycle: Principles of Control*. 1st ed. New Science Press; 2007.
9. Pomerening JR. Positive-feedback loops in cell cycle progression. *FEBS Lett*. 2009;583(21):3388-3396.
10. Ferrell JE. Feedback loops and reciprocal regulation: recurring motifs in the systems biology of the cell cycle. *Curr Opin Cell Biol*. 2013;25(6):676-686.
11. Santos SDM, Wollman R, Meyer T, Ferrell JE. Spatial positive feedback at the onset of mitosis. *Cell*. 2012;149(7):1500-1513.
12. Sha W, Moore J, Chen K, et al. Hysteresis drives cell-cycle transitions in Xenopus laevis egg extracts. *Proc Natl Acad Sci U S A*. 2003;100(3):975-980.
13. Pomerening JR, Sontag ED, Ferrell JE. Building a cell cycle oscillator: Hysteresis and bistability in the activation of Cdc2. *Nat Cell Biol*. 2003;5(4):346-351.
14. Izumi T, Walker DH, Maller JL. Periodic changes in phosphorylation of the Xenopus cdc25 phosphatase regulate its activity. *Mol Biol Cell*. 1992;3(8):927-939.
15. Kumagai A, Dunphy WG. Regulation of the cdc25 protein during the cell cycle in Xenopus extracts. *Cell*. 1992;70(1):139-151.
16. Tang Z, Coleman TR, Dunphy WG. Two distinct mechanisms for negative regulation of the Wee 1 protein kinase. *EMBO Journal*. 1993;12(9):3427-3436.
17. Mueller PR, Coleman TR, Dunphy WG. Cell cycle regulation of a Xenopus Wee1-like kinase. *Mol Biol Cell*. 1995;6(1):119-134.
18. McGowan CH, Russell P. Cell cycle regulation of human WEE1. *EMBO J*. 1995;14(10):2166-2175.

19. Araujo AR, Gelens L, Sheriff RSM, Santos SDM. Positive Feedback Keeps Duration of Mitosis Temporally Insulated from Upstream Cell-Cycle Events. *Mol Cell*. 2016;64(2):362-375.

20. Macedo JC, Vaz S, Bakker B, et al. FoxM1 repression during human aging leads to mitotic decline and aneuploidy-driven full senescence. *Nat Commun*. 2018;9(1):1-17.

21. Laoukili J, Alvarez M, Meijer LAT, et al. Activation of FoxM1 during G2 requires cyclin A/Cdk-dependent relief of autorepression by the FoxM1 N-terminal domain. *Mol Cell Biol*. 2008;28(9):3076-3087.

22. Leung TWC, Lin SSW, Tsang ACC, et al. Over-expression of FoxM1 stimulates cyclin B1 expression. *FEBS Lett*. 2001;507(1):59-66.

23. Fu Z, Malureanu L, Huang J, et al. Plk1-dependent phosphorylation of FoxM1 regulates a transcriptional programme required for mitotic progression. *Nat Cell Biol*. 2008;10(9):1076-1082.

24. Laoukili J, Alvarez-Fernandez M, Stahl M, Medema RH. FoxM1 is degraded at mitotic exit in a Cdh1-dependent manner. *Cell Cycle*. 2008;7(17):2720-2726.

25. Park HJ, Costa RH, Lau LF, Tyner AL, Raychaudhuri P. Anaphase-Promoting Complex/Cyclosome-Cdh1-Mediated Proteolysis of the Forkhead Box M1 Transcription Factor Is Critical for Regulated Entry into S Phase. *Mol Cell Biol*. 2008;28(17):5162-5171.

26. Ly DH, Lockhart DJ, Lerner RA, Schultz PG. Mitotic misregulation and human aging. *Science*. 2000;287(5462):2486-2492.

27. Ribeiro R, Macedo JC, Costa M, et al. In vivo cyclic induction of the FOXM1 transcription factor delays natural and progeroid aging phenotypes and extends healthspan. *Nat Aging*. 2022;2(5):397-411.

28. Bar-On O, Shapira M, Skorecki K, Hershko A, Hershko DD. Regulation of APC/CCdh1 ubiquitin ligase in differentiation of human embryonic stem cells. *Cell Cycle*. 2010;9(10):1986-1989.

29. Gieffers C, Peters BH, Kramer ER, Dotti CG, Peters JM. Expression of the CDH1-associated form of the anaphase-promoting complex in postmitotic neurons. *Proc Natl Acad Sci U S A*. 1999;96(20):11317-11322.

30. Almeida A, Bolaños JP, Moreno S. Cdh1/Hct1-APC is essential for the survival of postmitotic neurons. *Journal of Neuroscience*. 2005;25(36):8115-8121.

31. Liu DX, Greene LA. Neuronal apoptosis at the G1/S cell cycle checkpoint. *Cell Tissue Res*. 2001;305(2):217-229.

32. Barroso-Vilares M, Macedo JC, Reis M, Warren JD, Compton D, Logarinho E. Small-molecule inhibition of aging-associated chromosomal instability delays cellular senescence. *EMBO Rep*. 2020;21(5):e49248.

33. Grant GD, Kedziora KM, Limas JC, Cook JG, Purvis JE. Accurate delineation of cell cycle phase transitions in living cells with PIP-FUCCI. *Cell Cycle*. 2018;17(21-22):2496-2516.

34. Sakaue-Sawano A, Kurokawa H, Morimura T, et al. Visualizing Spatiotemporal Dynamics of Multicellular Cell-Cycle Progression. *Cell*. 2008;132(3):487-498.

35. Sakaue-Sawano A, Yo M, Komatsu N, et al. Genetically Encoded Tools for Optical Dissection of the Mammalian Cell Cycle. *Mol Cell*. 2017;68(3):626-640.

36. Sakaue-Sawano A, Miyawaki A. Visualizing spatiotemporal dynamics of multicellular cell-cycle progressions with fucci technology. *Cold Spring Harb Protoc*. 2014;2014(5):525-531.

37. Novák B, Tyson JJ. Numerical analysis of a comprehensive model of M-phase control in Xenopus oocyte extracts and intact embryos. *J Cell Sci*. 1993;106:1153-1168.

38. Pines J, Hunter T. Human cyclins A and B1 are differentially located in the cell and undergo cell cycle-dependent nuclear transport. *Trends Cell Biol*. 1992;2(1):1-17.

39. Gavet O, Pines J. Activation of cyclin B1-Cdk1 synchronizes events in the nucleus and the cytoplasm at mitosis. *J Cell Biol*. 2010;189(2):247-259.

40. Naylor RM, Baker DJ, Van Deursen JM. Senescent cells: a novel therapeutic target for aging and age-related diseases. *Clin Pharmacol Ther*. 2013;93(1):105-116.

41. MacNee W, Rabinovich RA, Choudhury G. Ageing and the border between health and Disease. *European Respiratory Journal*. 2014;44(5):1332-1352.

42. Prasad S, Sung B, Aggarwal BB. Age-Associated Chronic Diseases Require Age-Old Medicine: Role of Chronic Inflammation. *Prev Med (Baltim)*. 2012;54:S29-S37.

43. Partridge L. Intervening in ageing to prevent the diseases of ageing. *Trends Endocrinol Metab*. 2014;25(11):555-557.

44. Kirkwood TBL. Understanding the Odd Science of Aging. *Cell*. 2005;120(4):437-447.

45. White J, Dalton S. Cell cycle control of embryonic stem cells. *Stem Cell Rev*. 2005;1(2):131-138.

46. Calder A, Roth-Albin I, Bhatia S, et al. Lengthened G1 phase indicates differentiation status in human embryonic stem cells. *Stem Cells Dev*. 2013;22(2):279-295.

47. Becker KA, Stein JL, Lian JB, Van Wijnen AJ, Stein GS. Human embryonic stem cells are pre-mitotically committed to self-renewal and acquire a lengthened G1 phase upon lineage programming. *J Cell Physiol*. 2010;222(1):103-110.

48. Weinert TA, Hartwell LH. The RAD9 Gene Controls the Cell Cycle Response to DNA Damage in Saccharomyces cerevisiae. *Science*. 1988;241(4863):317-322.

49. Hartwell LH, Weinert TA. Checkpoints: Controls That Ensure the Order of Cell Cycle Events. *Science*. 1989;246(4930):629-634.

50. Amon A, Tyers M, Futcher B, Nasmyth K. Mechanisms that help the yeast cell cycle clock tick: G2 cyclins transcriptionally activate G2 cyclins and repress G1 cyclins. *Cell*. 1993;74(6):993-1007.

51. Minshull J, Golsteyn R, Hill CS, Hunt T. The A- and B-type cyclin associated cdc2 kinases in Xenopus turn on and off at different times in the cell cycle. *EMBO J*. 1990;9(9):2865-2875.

52. Murray AW, Kirschner MW. Dominoes and clocks: The union of two views of the cell cycle. *Science*. 1989;246(4930):614-621.

53. Surana U, Robitsch H, Price C, et al. The role of CDC28 and cyclins during mitosis in the budding yeast S. cerevisiae. *Cell*. 1991;65(1):145-161.

54. Coudreuse D, Nurse P. Driving the cell cycle with a minimal CDK control network. *Nature*. 2010;468(7327):1074-1079.

55. Stern B, Nurse P. A quantitative model for the cdc2 control of S phase and mitosis in fission yeast. *Trends in Genetics*. 1996;12(9):345-350.

56. Swaffer MP, Jones AW, Flynn HR, Snijders AP, Nurse P. CDK Substrate Phosphorylation and Ordering the Cell Cycle. *Cell*. 2016;167(7):1750-1761.

57. Queralt E, Uhlmann F. Cdk-counteracting phosphatases unlock mitotic exit. *Curr Opin Cell Biol*. 2008;20(6):661-668.

58. Bouchoux C, Uhlmann F. A Quantitative Model for Ordered Cdk Substrate Dephosphorylation during Mitotic Exit. *Cell*. 2011;147(4):803-814.

59. Visintin R, Craig K, Hwang ES, Prinz S, Tyers M, Amon A. The Phosphatase Cdc14 Triggers Mitotic Exit by Reversal of Cdk-Dependent Phosphorylation. *Mol Cell*. 1998;2(6):709-718.

60. Wolf F, Wandke C, Isenberg N, Geley S. Dose-dependent effects of stable cyclin B1 on progression through mitosis in human cells. *EMBO J*. 2006;25(12):2802-2813.

61. Basu S, Greenwood J, Jones AW, Nurse P. Core control principles of the eukaryotic cell cycle. *Nature*. 2022;607(7918):381-386.

62. Spencer SL, Cappell SD, Tsai FC, Overton KW, Wang CL, Meyer T. The proliferation-quiescence decision is controlled by a bifurcation in CDK2 activity at mitotic exit. *Cell*. 2013;155(2):369-383.

63. Novak B, Tyson JJ. Mitotic kinase oscillation governs the latching of cell cycle switches. *Curr Biol*. 2022;32(12):2780-2785.

64. Rombouts J, Gelens L. Dynamic bistable switches enhance robustness and accuracy of cell cycle transitions. *PLoS Comput Biol*. 2021;17(1):e1008231.

65. Stallaert W, Kedziora KM, Chao HX, Purvis JE. Bistable switches as integrators and actuators during cell cycle progression. *FEBS Lett*. 2019;593(20):2805-2816.

66. Holt LJ, Krutchinsky AN, Morgan DO. Positive feedback sharpens the anaphase switch. *Nature*. 2008;454(7202):353-357.

67. Santos SDM, Ferrell JE. Systems biology: On the cell cycle and its switches. *Nature*. 2008;454(7202):288-289.

68. Rodier F, Campisi J. Four faces of cellular senescence. *J Cell Biol*. 2011;192(4):547-556.

69. Hernandez-Segura A, Nehme J, Demaria M. Hallmarks of Cellular Senescence. *Trends Cell Biol*. 2018;28(6):436-453.

70. Hernandez-Segura A, de Jong T V., Melov S, Guryev V, Campisi J, Demaria M. Unmasking Transcriptional Heterogeneity in Senescent Cells. *Curr Biol*. 2017;27(17):2652-2660.

71. González-Gualda E, Baker AG, Fruk L, Muñoz-Espín D. A guide to assessing cellular senescence in vitro and in vivo. *FEBS Journal*. 2021;288(1):56-80.

72. Ballabeni A, Park IH, Zhao R, et al. Cell cycle adaptations of embryonic stem cells. *Proc Natl Acad Sci U S A*. 2011;108(48):19252-19257.

73. Padgett J, Santos SDM. From clocks to dominoes: lessons on cell cycle remodelling from embryonic stem cells. *FEBS Lett*. 2020;594(13):2031-2045.

74. Harashima H, Dissmeyer N, Schnittger A. Cell cycle control across the eukaryotic kingdom. *Trends Cell Biol*. 2013;23(7):345-356.

75. Cross FR, Buchler NE, Skotheim JM. Evolution of networks and sequences in eukaryotic cell cycle control. *Philos Trans R Soc B: Biol Sci*. 2011;366(1584):3532-3544.

76. Cao L, Chen F, Yang X, Xu W, Xie J, Yu L. Phylogenetic analysis of CDK and cyclin proteins in premetazoan lineages. *BMC Evol Biol*. 2014;14(1):1-16.

77. Alon U. Network motifs: theory and experimental approaches. *Nat Rev Genet*. 2007;8(6):450-461.

78. Ferrell JE. Self-perpetuating states in signal transduction: positive feedback, double-negative feedback and bistability. *Curr Opin Cell Biol*. 2002;14(2):140-148.

79. Gérard C, Gonze D, Goldbeter A. Effect of positive feedback loops on the robustness of oscillations in the network of cyclin-dependent kinases driving the mammalian cell cycle. *FEBS J*. 2012;279(18):3411-3431.

80. López-Avilés S, Kapuy O, Novák B, Uhlmann F. Irreversibility of mitotic exit is the consequence of systems-level feedback. *Nature*. 2009;459(7246):592-595.

81. Skotheim JM, Di Talia S, Siggia ED, Cross FR. Positive feedback of G1 cyclins ensures coherent cell cycle entry. *Nature*. 2008;454(7202):291-296.

82. Van Deursen JM. Senolytic therapies for healthy longevity. *Science*. 2019;364(6441):636-637.

83. Zhang P, Kishimoto Y, Grammatikakis I, et al. Senolytic therapy alleviates Aβ-associated oligodendrocyte progenitor cell senescence and cognitive deficits in an Alzheimer's disease model. *Nat Neurosci*. 2019;22(5):719-728.

84. Novais EJ, Tran VA, Johnston SN, et al. Long-term treatment with senolytic drugs Dasatinib and Quercetin ameliorates age-dependent intervertebral disc degeneration in mice. *Nat Commun*. 2021;12(1):1-17.

85. Suda M, Shimizu I, Katsuumi G, et al. Senolytic vaccination improves normal and pathological age-related phenotypes and increases lifespan in progeroid mice. *Nat Aging*. 2021;1(12):1117-1126.

86. Mosteiro L, Pantoja C, Alcazar N, et al. Tissue damage and senescence provide critical signals for cellular reprogramming in vivo. *Science*. 2016;354(6315):aaf4445.

87. Antelo-Iglesias L, Picallos-Rabina P, Estévez-Souto V, Da Silva-Álvarez S, Collado M. The role of cellular senescence in tissue repair and regeneration. *Mech Ageing Dev*. 2021;198:111528.

88. Jun J Il, Lau LF. The matricellular protein CCN1 induces fibroblast senescence and restricts fibrosis in cutaneous wound healing. *Nat Cell Biol*. 2010;12(7):676-685.

89. Demaria M, Ohtani N, Youssef SA, et al. An Essential Role for Senescent Cells in Optimal Wound Healing through Secretion of PDGF-AA. *Dev Cell*. 2014;31(6):722-733.